Integrated Study of MFRSR-Derived Parameters of Atmospheric Aerosols and Trace Gases Over the ARM Cloud and Radiation Testbed (CART) Site Extended Facilities

M. D. Alexandrov and B. Cairns
Columbia University
National Aeronautics and Space Administration
Goddard Institute for Space Studies
New York, New York

A. A. Lacis and B. E. Carlson
National Aeronautics and Space Administration
Goddard Institute for Space Studies
New York, New York

Introduction

We present results of a preliminary analysis of the multi-instrument multifilter rotating shadowband radiometer (MFRSR) dataset from Atmospheric Radiation Measurement (ARM) Program Cloud and Radiation Testbed (CART) extended facilities (EF) site aimed at determining spatial distributions of aerosol parameters in addition to their temporal variability. The MFRSR network at the Southern Great Plains (SGP) site consists of 21 instruments arrayed across approximately 55,000 square miles (3 degrees by 4 degrees). The first data from SGP central facility MFRSR became available in 1993; since then the number of EF instruments gradually increased.

Aerosols at the SGP site come from both local and remote sources including agricultural activities, pollutions from industrial areas, fire smoke, and even Sahara dust. As a test dataset for this study we chose data from May 1998 that includes the well-documented Central America's fire smoke transport event (Peppler et al. 2000). However in the preliminary testing reported here, we use the data obtained by 15 MFRSRs (located at EF 1 to 5, 7, 8, 10, 11, 15, 16, 20, 22, 24, and 25) on May 4, 1998, when smoke over SGP was not reported and measured optical depths were moderate (unlike, for example, May 13).

The single-instrument retrievals were made according to our previously reported method (Alexandrov et al. 1999). They include daily time series of the column mean aerosol particle size, aerosol optical depth, NO_2, and ozone column amounts. On the first step, we concentrate on network retrievals of the quantities, the determination of which requires minimum assumptions: Aerosol optical depth (AOD) at 870 nm, and direct-to-diffuse ratio (DDR) at the same wavelength. MFRSR data is sampled at a number of locations during daytime. The used intervals may be different for different sites depending on local cloud cover and possibly on instrument functioning problems (e.g., segments with pronounced

misalignment should be excluded). Thus, the number of data points on the map may change throughout the same day, and one of the requirements to the interpolation scheme is to minimize the effect of such data reduction on the output fields.

The density of EF MFRSR sites allows combining the retrievals from individual instruments into a series of two-dimensional (2D) images. We explore a variety of interpolation techniques, such as weighted averaging, spline interpolations, and (ordinary) kriging. We also consider coupling of these interpolation methods with simple atmospheric transport algorithms using meteorological data, such as the ground winds measured at the most of EF 24 hours a day with 1 min intervals. The set of sites with available wind data, however, may not exactly coincide with the set of the MFRSR sites used on a particular day. We assume that AOD, being an integral of the aerosol concentration, is transported with the air masses by winds. At this moment, we use the winds measured at the ground and neglect the altitude dependence of the wind speed. A thin plate spline method is used for interpolation of the wind field. Direct-to-diffuse ratio depends not only on AOD, but also on the solar zenith angle, thus it cannot be directly transported. However, maps of this calibration-independent parameter still provide a qualitative picture of atmospheric processes in the area (Peppler et al. 2000).

Figure 1 shows a series of AOD maps made with 1-hr temporal resolution. The presented AOD is retrieved from 870 nm channel. To construct these images while reducing sensitivity to the changing number of sites (data from a small number of them were not usable in the early morning and later afternoon parts due to alignment problems), we use the following method. We consider the values obtained at each site at the moment to which the map is referenced, as well as the values taken at 5 moments in the future and 5 moments in the past (1, 2, …, and 5 hours from the present moment; the number of points and their time spacing may vary depending on atmospheric conditions). Then we use time-dependent wind fields to transport past values along the winds and the future values against the winds. The 11-point traces obtained in this way are then used for interpolation. The structure of such a dataset is characterized by much shorter spacing along the wind than in the across-wind direction. This substantially reduces applicability of spline techniques, in particular, when traces from different sites come close to each other with values slightly different due to transport and measurement uncertainties. In such cases, spline produces high derivatives leading to unrealistic maxima and minima in the areas with a low number of the sampling points. However, as shown in Figure 1, the simple inversed-distance weighted averaging technique still provides a realistic interpolation.

Comparison between values transported from different sites to the same (or close) locations provides a good intercomparison check that may lead to improving each instrument calibration and retrieval assumptions. Both measurement accuracy and interpolation algorithm performance are being evaluated by the widely used geostatistical procedure. We delete one site from the network, predict the time series of measured values at its location using the rest of the network data, and then compare the predicted values with the actual measurements at the deleted site. The differences in optical depth obtained in this way range from 0.01 to 0.05 depending on the site location and variability of aerosol load (averaging tends to reduce this variability). We hope to improve the prediction accuracy in further development of the interpolation algorithm.

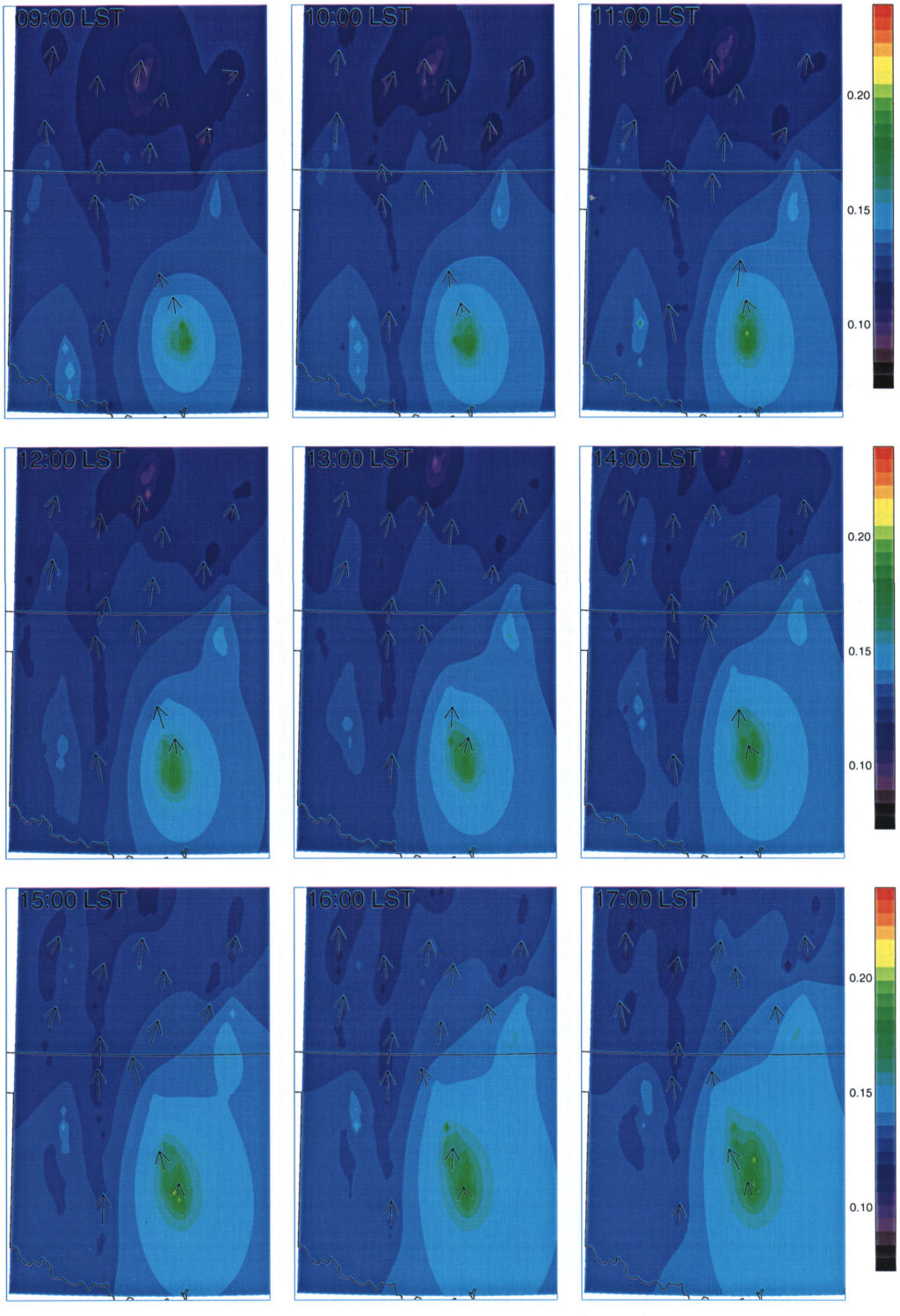

Figure 1. Time series of AOD (at 870 nm) maps constructed based on MFRSR measurements at SGP EF made on May 4, 1998. Local surface winds are depicted by arrows.

Construction of 2D images using ground-based remote sensing measurements may have a natural application to validation of satellite retrievals of atmospheric properties, as well as to atmospheric correction of satellite observations of land surface. Satellite retrievals provide a value of a measured physical parameter (e.g., AOD) averaged over the viewing footstep (e.g., about 1 degree by 1 degree, like for Total Ozone Mapping Experiment Spectrometer [TOMS] observations) at the particular moment when the satellite overpasses the site. The intercomparison between these measurements and continuous but local ground-based retrievals requires not only construction of a smooth interpolated image described above, but also a statistical study of high-frequency spatial variability, which may affect the averaging over the satellite footprint. To address this issue, we follow the approach currently used in cloud remote sensing (see for example, Lovejoy et al. 1993, Feijt and Jonker 2000) and construct variance spectra of AOD time series. They may be converted to spatial structure spectra using a factor depending on the mean wind speed. These spectra reflect the structure of atmospheric turbulence and usually have power law form (scale invariance). A traditional model of atmospheric turbulence predicts two main regimes with different power law spectra: Large-scale 2D turbulence (with the power exponent -3) and small-scale three-dimensional turbulence (with the power exponent -5/3, approximately -1.67). However, in more complicated real situations, the actual values of power exponents may deviate from the theoretically predicted ones. Our analysis of the SGP data from May 4, 1998, shows general agreement with this model and with power exponents obtained for clouds: Our high-frequency exponents range from -1.91 to -1.15, while the low-frequency exponents (when pronounced) range from -3.71 to -2.74.

References

Alexandrov, M., A. Lacis, B. Carlson, and B. Cairns, 1999a: Remote sensing of atmospheric aerosols, nitrogen dioxide, and ozone by means of multi-filter rotating shadow-band radiometer. In *Remote Sensing of Clouds and Atmosphere*, J. Russell and C. Serio, Eds, Proc. SPIE 3867, 156-170.

Feijt, A., H. Jonker, 2000: Comparison of scaling parameters from spatial and temporal distributions of cloud properties. *J. Geophys. Res.*, **105**, 29,089-29,097.

Lovejoy, S., D. Schertzer, P. Silas, Y. Tessier, and D. Lavalee, 1993: The unified scaling model of atmospheric dynamics and systematic analysis of scale invariance in cloud radiances. *Ann. Geophysicae*, **11**, 119-127.

Peppler, R. A., C. P. Bahrmann, J. C. Barnard, J. R. Campbell, M. D. Cheng, R. A. Ferrare, R. N. Halthore, L. A. Heilman, D. L. Hlavka, N. S. Laulainen, C. J. Lin, J. A. Ogren, M. R. Poellot, L. A. Remer, K. Sassen, J. D. Spinhirne, M. E. Splitt, and D. D. Turner, 2000: ARM Southern Great Plains site observations of the smoke pall associated with the 1998 Central American fires. *B. Am. Meteorol. Soc.*, **81**, 2563-2591.